



Chinese Pharmaceutical Association
Institute of Materia Medica, Chinese Academy of Medical Sciences

Acta Pharmaceutica Sinica B

www.elsevier.com/locate/apsb
www.sciencedirect.com



ORIGINAL ARTICLE

A non-human primate derived anti-P-selectin glycoprotein ligand-1 antibody curtails acute pancreatitis by alleviating the inflammatory responses



Yuhan Li^{a,b,†}, Xiangqing Ding^{c,†}, Xianxian Wu^{a,†}, Longfei Ding^d,
Yuhui Yang^e, Xiaoliang Jiang^a, Xing Liu^a, Xu Zhang^f, Jianrong Su^b,
Jianqing Xu^{c,g,*}, Zhiwei Yang^{a,*}

^aInstitute of Laboratory Animal Science, Chinese Academy of Medical Sciences (CAMS) & Comparative Medicine Centre, Peking Union Medical College (PUMC), Beijing 100021, China

^bDepartment of Clinical Laboratory, Beijing Friendship Hospital, Capital Medical University, Beijing 100050, China

^cShanghai Sinobay Biotechnology Company (Limited), Shanghai 201500, China

^dShanghai Public Health Clinical Center, Fudan University, Shanghai 200083, China

^eCapital Medical University, Beijing 100069, China

^fDepartment of Hepatobiliary Pancreatic Surgery, Zhengzhou University People's Hospital, Henan Provincial People's Hospital, Zhengzhou 450003, China

^gChongqing Institutes for Life Science Innovation, Chongqing 400715, China

Received 11 May 2023; received in revised form 4 July 2023; accepted 10 July 2023

KEY WORDS

Acute pancreatitis;
PSGL-1;
Non-human primate;
Monoclonal antibody;
Therapeutic antibody
RH001-6;

Abstract Acute pancreatitis (AP) is a devastating disease characterized by an inflammatory disorder of the pancreas. P-selectin glycoprotein ligand-1 (PSGL-1) plays a crucial role in the initial steps of the adhesive at process to inflammatory sites, blockade of PSGL-1 might confer potent anti-inflammatory effects. In this study, we generated two non-human primate derived monoclonal antibodies capable of efficiently targeting human PSGL-1, RH001-6 and RH001-22, which were screened from immunized rhesus macaques. We found that RH001-6, can effectively block the binding of P-selectin to PSGL-1, and abolish the adhesion of leukocytes to endothelial cells *in vitro*. *In vivo*, we verified that RH001-6 relieved

*Corresponding authors.

E-mail addresses: yangzhiwei@nilas.pumc.edu.cn (Zhiwei Yang), xujianqing@fudan.edu.cn (Jianqing Xu).

†This authors made equal contributions to this work.

Peer review under the responsibility of Chinese Pharmaceutical Association and Institute of Materia Medica, Chinese Academy of Medical Sciences.

<https://doi.org/10.1016/j.apsb.2023.07.028>

2211-3835 © 2023 Chinese Pharmaceutical Association and Institute of Materia Medica, Chinese Academy of Medical Sciences. Production and hosting by Elsevier B.V. This is an open access article under the CC BY-NC-ND license (<http://creativecommons.org/licenses/by-nc-nd/4.0/>).

Adhesion of leukocytes to endothelial cells;
Inflammatory responses;
Pancreatic injury

inflammatory responses and pancreatic injury in both caerulein and L-arginine induced AP models. We also evaluated the safety profile after RH001-6 treatment in mice, and verified that RH001-6 did not cause any significant pathological damages *in vivo*. Taken together, we developed a novel non-human primate derived PSGL-1 blocking antibody with high-specificity, named RH001-6, which can interrupt the binding of PSGL-1 and P-selectin and attenuate inflammatory responses during AP. Therefore, RH001-6 is highly potential to be further developed into therapeutics against acute inflammatory diseases, such as AP.

© 2023 Chinese Pharmaceutical Association and Institute of Materia Medica, Chinese Academy of Medical Sciences. Production and hosting by Elsevier B.V. This is an open access article under the CC BY-NC-ND license (<http://creativecommons.org/licenses/by-nc-nd/4.0/>).

1. Introduction

Acute pancreatitis (AP) is an acute inflammatory process of the pancreas, starting with premature activation of digestive proteases in pancreatic gland cells, causing pancreatic cell damage, swelling, and inflammatory cellular infiltration^{1,2}. The variable course of the disease and its uncertain pathophysiological mechanism undermined the development of therapeutic agents for AP. Although most AP patients experience a mild and self-limiting course, about 20% of patients develop into severe AP, with a high mortality rate³. Despite decades of efforts, there remains no effective drug for AP⁴. AP is characterized by pancreatic self-digestion in pancreatic acinar cells (PACs)⁵, which causes inflammation, edema, and injury of the pancreas. The damaged PACs release a series of pro-inflammatory factors, leading to local and systemic inflammatory response syndrome⁶, and resulting in multi-system organ failure, is the primary cause of death. Therefore, developing safe and effective drugs to restrain inflammation is a paramount objective for AP treatment.

PSGL-1, a type I transmembrane mucin on leukocytes, is formed from two 120 K_D homologous sialic acidified subunit proteins through disulfide bonding⁷. PSGL-1 is mainly expressed on the leukocyte membrane, and mediates leukocyte rolling and adhesion by binding to activated P-, E-, and L-selectins, which is the crucial process in initial step of the inflammation^{8–11}. In recent years, it has been demonstrated that inhibition of PSGL-1 plays a beneficial role in a broad spectrum of inflammatory diseases, including atherosclerosis, obesity, ischemia-reperfusion injury, peritonitis, thrombosis, allergic diseases, and autoimmune diseases^{12–19}. However, currently no anti-PSGL-1 antibody drug available for clinical practice. There are two kinds of antibodies against PSGL-1 in clinical phase II trials, including KPL1 and 2PH1, which target type I diabetes, transplanted anti-main disease, psoriasis, psoriasis arthritis, ulcerative colon inflammation and venous thromboembolism, asthma, chronic obstructive pulmonary disease, or Crohn's disease indications^{20–23}. All these diseases are related to PSGL-1 mediated intravascular rolling or tethering of leukocytes and recruitment to inflammatory sites. Moreover, our recent studies have shown that the deficiency of PSGL-1 prevented AP and aortic aneurysm formation in established animal models by interrupting leukocyte and endothelial cell adhesion and inflammation^{16,19}. Thus, blocking PSGL-1 is likely to be a promising anti-inflammatory strategy.

In this study, we developed two novel monoclonal antibodies (mAbs) against PSGL-1, RH001-6 and RH001-22 (Patent number: 2021109591435), from human PSGL-1 immunized non-human primate, and focused on their roles in the treatment of AP. We first verified that both RH001-6 and RH001-22 can block the binding

of P-selectin and PSGL-1 *in vitro* and thereby eliminating the adhesion between leukocytes and endothelial cells. Compared with RH001-22, RH001-6 has higher affinity for human PSGL-1 and the ability to block the combination of P-selectin and PSGL-1. Therefore, we then further demonstrated that RH001-6 can more effectively block the interaction between P-selectin and PSGL-1, protect AP from pancreas inflammatory injury and ameliorate disease severity. Overall, a non-human primate derived anti-PSGL-1 mAb RH001-6, is high potential to be developed as effective therapeutics for AP.

2. Materials and methods

2.1. Design and production of DNA, K562 based vaccine and protein vaccines

DNA vaccines expressing P-selectin glycoprotein ligand-1 (PSGL-1) and PSGL-1 (ECD)-HuIgG2 Fc were constructed by cloning the target genes into the pVRCSV1.0 vector (Addgene). The immunogen expression by the DNA vectors were verified by transient transfection of HEK293T cells, and were examined by flow cytometry following PSGL-1 staining. Then, PSGL-1 (ECD)-HuIgG2 Fc of the resultant cell lysate harvested 48 h were analyzed by Western blotting using HRP-goat anti-human IgG1. Construction, and verification of K562 cells-PSGL-1 based vaccine was described in detail in the methods²⁴. Briefly, codon-optimized DNA sequences encoding PSGL-1 were synthesized (Generay Biotech Co., Ltd.), and cloned into pHAGE-puro lentiviral vector (Addgene) to generate pHAGE-PSGL-1-puro plasmid. Polybrene mediated transduction of K562 cells with the resultant lentivirus stock was performed in 12-well format by centrifugation at $1000 \times g$ for 2 h at 32 °C. The cells that remained after puromycin selection were subjected to single-cell sorting by flow cytometry based on recognition by human PSGL-1 protein and sorted by a FACSAriaIII cytometer (BD Biosciences). Cells were counted and following collection by centrifugation, re-suspended to a final concentration of 1×10^7 cells/mL. The inactivation of K562 cells-PSGL-1 were achieved either by formalin fixation. Cells were counted and collected by centrifugation, suspended in 1% formalin to a final concentration of 1×10^7 cells/mL. After being fixed for 10 min at room temperature, the cells were washed 4 times with PBS to remove the residual formalin.

2.2. Immunization of Rhesus macaques

For the immunization of *Rhesus macaques*, all vaccines were intramuscularly injected into the leg muscle and the volume per administration was 1 mL. The amount of vaccine per

administration for DNA was 1 mg. The 1×10^7 K562 cells-PSGL-1 were subcutaneously injected into the left leg muscle. The PSGL-1 (ECD)-HuIgG2 Fc protein was adjuvant with an equal volume of alum shortly before application at a final protein concentration of 0.1 mg/mL, achieving 100 μ g per immunization, were subcutaneously injected into the right leg muscle. Blood samples were harvested after 2 weeks of each immunization to evaluate PSGL-1-specific antibody response. All *Rhesus macaques* were maintained under specific pathogen-free conditions following the Association for Assessment and Accreditation of Laboratory *Rhesus macaques* with approval from the Institutional Animal Care and Use Committee (IACUC) of Shanghai Public Health Clinical Center (Shanghai, China). The research was conducted in compliance with the Animal Welfare Act, adhering to the principles stated in the Guide for the Care and Use of Laboratory Animals, NRC Publication, 2011 edition. NE. Rep.

2.3. Antigen specific memory B cells isolation and culturing in vitro

For cell surface staining, fresh peripheral blood mononuclear cells (PBMCs) were suspended in 100 μ L of FACS staining buffer (2% FBS in PBS) containing antibody reagents anti-CD3 (PB), anti-CD14 (APC), anti-CD20 (PE), anti-CD27 (APC-H7), anti-IgG (PE-Cy7), and Alexa Fluor[®] 488 labeled PSGL-1 (ECD)-HuIgG2 Fc protein following Alexa Fluor[™] 488 protein labeling kit protocol (Invitrogen), and incubated for 30 min at 4 °C. The stained cells were analyzed and sorted by FACS Aria III cytometer into 96-well plates containing IL-2, IL-21 and irradiated 3T3-msCD40L feeder cells according to the gating strategy at a density of 4 cells per well²⁵. After 13 days of incubation, supernatants from each well were screened for ELISA assay.

2.4. Antibody cloning, sequencing, and production

First-round and second-round polymerase chain reaction (PCR) primers were designed based on published *Rhesus macaques* germline sequences study (Supporting Information Tables S1 and S2)²⁶. Reverse transcription was carried out using the Super-Script[™] III Cell Direct cDNA Synthesis kit (Invitrogen) according to the manufacturer's instructions. PCR products were generated with the PrimeSTAR[™] GXL DNA polymerase (Clontech). IG variable domain genes were amplified from 2 μ L cDNA by nested PCR. Cloning was carried out using the C112-ClonExpress-II One Step Cloning Kit (Vazyme Biotech). Briefly, 50 ng purified PCR products were mixed with 1 μ L C112-ClonExpress-II enzyme premix and 100 ng linearized vector. Water was added up to a total volume of 10 μ L. The reaction was incubated for 30 min at 37 °C, and then placed on ice. All products were used for TOP10 competent *E. coli* transformation. Eight colonies for each product were picked for sequencing confirmation. Genes encoding Ig VH, Ig V κ and V λ were cloned into IgG heavy- and light-chains expression vectors and expressed by transfection of HEK293T cells and purification by protein G has been described previously²⁶. Briefly, equal molar amounts of heavy- and light-chains plasmids were co-transfected into HEK293T cells for transient expression with TrueFect[™] reagent (Polyplus). The supernatants were harvested at 4 days after transfection. The full-length IgG was purified using a recombinant protein G column (GE Healthcare).

2.5. Measurement of binding affinity between anti-PSGL-1 antibodies with human PSGL-1 antigen

The apparent binding affinity of RH001-6 and RH001-22 to human PSGL-1 were determined at 25 °C by surface plasmon resonance (SRP) using Series Sensor Chip Protein A (Pro A) that were loaded with 20 μ g/mL RH001-6 or RH001-22 in running buffer, set the flow rate to 10 μ L/min, capture about 2000 Response (RU). Association curves were recorded for 5 min by incubating the monoclonal antibody (mAb)-coated sensors with different concentrations of human PSGL-1.

Measurement of apparent K_D for RH001-6 was determined using Series Sensor Chip CM5. The human PSGL-1 antigen (Sino Biological) was diluted to 200 nmol/L with acetate (pH 5.0), RH001-6 adjusted to 1000 nmol/L with $1 \times$ HBS-EP+(pH 7.4) buffer. After diluting to 62.5, 31.25, 15.625, 7.8125, 3.906, and 1.953 nmol/L, respectively, the flow rate was set to 30 μ L/min, the combination time to 180 s, the dissociation time to 300 s, the default reaction temperature to 25 °C, and then detection was conducted. When the following conditions are met simultaneously, the result is reliable: $\text{Chi}^2 \leq 10\% \times R_{\text{max}}$.

2.6. Cell culture and adhesion assay

The human umbilical vein endothelial cells (HUVECs) were cultured in endothelial cell culture medium containing 10% fetal bovine serum (FBS), 1% endothelial cell growth factor and 1% penicillin/streptomycin (P/S). Monocyte line cells of human peripheral blood (THP-1 cells) were prepared in RPMI-1640 medium containing 10% FBS and 1% P/S. Cells were placed in 37 °C, 5% CO₂ cell incubator. THP-1 cells were incubated with 1, 5, and 10 μ g/mL of blocking monoclonal antibodies (mAbs) to human PSGL-1, RH001-6, RH001-22 and KPL1²⁷ (Santa Cruz Biotechnology) and mouse PSGL-1, 4RA10²⁸ (BD, Bioscience Pharmingen) for 24 h, and then were stained with green 5-chloromethylformacein diacetate (CMFDA) (Abcam) for 30 min at 37 °C and then purified 3 times using PBS. The stained THP-1 cells were incubated together with prepared HUVEC cells at 37 °C, 5% CO₂ cell incubator for 1 h. The non-adherent cells were removed using PBS. The adherent THP-1 cells to endothelial cells were analyzed with fluorescence microscope and were counted by ImageJ software. The inhibition efficiency was calculated using Eq. (1):

$$\text{Inhibition efficiency (\%)} = (1 - \frac{\text{the number of leukocytes adhered in the experimental group}}{\text{the number of leukocytes adhered in the control group}}) \times 100 \quad (1)$$

2.7. RH001-6 blocking PSGL-1 and P-selectin binding ability

THP-1 cells suspension was incubated with the purified rat anti-human CD16/CD32 (Mouse BD Fc block reagent) for 30 min at room temperature to block the Fc fragment, followed by PBS termination and centrifugation at 2000 rpm for 5 min at 4 °C. After that, THP-1 cells were suspended by 100 μ L PBS and then incubated with recombinant human P-selectin (CD62P) Fc chimera in the presence of RH001-6, RH001-22, KPL1 and 4RA10 or not for 30 min. Subsequently, THP-1 cells were washed twice using PBS, and then were incubated with APC-Cy7-conjugated anti-CD45 and BV605-conjugated anti-CD62P for

30 min on ice. The percentage of CD62P⁺CD45⁺/total CD45⁺ cells was analyzed using flow cytometry.

2.8. Animal experiments

Male BALB/c nude mice and C57BL/6J mice (6–8 weeks old, 18–20 g) were purchased from Beijing HFK Bioscience Co., Ltd. (Beijing, China). Mice were housed in a temperature- and light/dark cycle-controlled environment with free access to standard rodent chow and water. Animals were adapted to the environment for 7 days before starting experiments. All animal studies were approved by the Animal Care and Use Committee at the Institute of Laboratory Animal Science, Chinese Academy of Medical Sciences and Peking Union Medical College (YZW20190001), and conformed to the guidelines from Directive 2010/63/EU of the European Parliament on the protection of animals used for scientific purposes.

2.9. Induction of experimental acute pancreatitis mouse model and drug treatment

Acute pancreatitis (AP) was induced by intraperitoneal (i.p.) injections of 0.2 mg/kg caerulein (Sigma) into BALB/c nude mice, continuous injection for 7 times, with an interval of 1 h each time, and i.p. injection of 10 mg/kg lipopolysaccharide (LPS) (Sigma) at the same time during the last injection of caerulein. All mice were randomly divided into five groups. One control group ($n = 6$), which only received repetitive i.p. injection of normal saline (NS). The other four groups were i.p. injections of caerulein plus LPS to prepare AP mouse model (caerulein, $n = 6$), isotype control antibody (IgG1, 10 mg/kg, BD Bioscience Pharmingen, $n = 6$) and anti-PSGL-1 antibodies RH001-6 or 4RA10 (10 mg/kg, $n = 6$) by tail intravenous injection at 8, 12 and 24 h after the first dose of caerulein injection. The animals were sacrificed 48 h after the first dose of caerulein injection.

The second experimental AP model was induced in C57BL/6J mice by i.p. injections of L-arginine twice, with the concentration of 4 g/kg body weight, and the interval between injections of 1 h²⁹. The control group received similar injections of NS. Isotype control antibody (IgG1, 10 mg/kg, $n = 6$) and anti-PSGL-1 antibodies RH001-6 or 4RA10 (10 mg/kg, $n = 6$) were administered to the mice by tail intravenous injection at 8, 12 and 24 h after the first dose of L-arginine injection. Mice were sacrificed 48 h after the first i.p. injection of L-arginine.

At the end of the treatment, the animals were sacrificed in deep anesthesia using isoflurane (1.5%–2.5%, inhaled). The abdomen was opened by a longitudinal incision and blood were collected from the inferior vena cava. The pancreatic tissues were collected, and a small portion were fixed in 10% neutral buffer formalin and embedded in paraffin, and the remaining part were frozen in liquid nitrogen.

2.10. Histological, immunohistochemically and immunofluorescence staining

The pancreatic tissues embedded in paraffin were subjected to sections. Sections were stained with hematoxylin–eosin (H&E) to assess inflammatory cells infiltration and histopathological damage in mouse pancreatic tissue. Pancreatic injury score was defined according to edema, hemorrhage, inflammatory cell infiltration and necrosis³⁰. For immunohistochemical analysis, the tissue sections were blocked in goat serum for 1 h and

then incubated with primary antibodies including anti-MPO (Proteintech, #22225-1-AP) and anti-F4/80 (Proteintech, #27044-1-AP) at a dilution of 1:200 at 4 °C overnight. Slices were washed with PBS, followed by using a general-purpose two-step test kit (ZSGB-BIO, #PV-900) according to the manufacturer's manual. After 3,3'-diaminobenzidine solution were incubated for 1 min and counterstained with hematoxylin. For immunofluorescence analysis, the pancreatic tissues were stained with anti-p65 (CST, #8242), anti-MPO (Abcam, #ab300650) and anti CD-68 (Abcam, #ab201340), followed by goat anti-rabbit IgG H&L (Alexa Fluor[®] 488) (Abcam, #ab150081) or goat anti-mouse IgG H&L (Alexa Fluor[®] 568) (Abcam, #ab175473) antibody at 1:2000 dilution and the nuclear counterstaining with DAPI. Images were photographed and digitized using an image scanner (Zeiss AxioScan.Z1, Zeiss; Olympus IX70, Leica).

2.11. Flow cytometry

The peripheral blood of mice was lysed using 1 × BD FACS lysis, and stained with the fluorescent labeling antibody to identify the percentage of monocytes and neutrophils that accounted for leukocytes. The antibodies involved in the experiment include anti-CD45 (APC-Cy7), anti-CD11b (Percp-Cy5.5), anti-Ly6c (FITC) and anti-Ly6g (APC). Cell fluorescence is quantified to the average fluorescence intensity or percentage of double-positive cells per time point. All results are analyzed by BD FACS Diva software.

2.12. ELISA assays

The level of inflammatory cytokines Th1 (Interferon- γ , IFN- γ ; Tumor necrosis factor- α , TNF- α) and Th17 (Interleukin-6, IL-6) in plasma were detected using an enzyme-linked immunosorbent assay. Mouse IFN- γ enzyme-linked immunosorbent test kit (Abcam, #ab267580), mouse TNF- α enzyme-linked immunosorbent test kit (Abcam, #ab208348) and mouse IL-6 enzyme-linked immunosorbent assay kit (Abcam, #ab100712) were used. Briefly, serum was added to a 96-well plate coated with IFN- γ , TNF- α , or IL-6 mAbs. After incubation for 2 h at 37 °C, the plate was washed 4 times with washing solution. Then, a bacterial hydrogenase solution was incubated with horseradish peroxidase for 30 min at 37 °C in the dark chamber. The activities of serum amylase were measured by enzyme dynamics chemistry using commercial kits according to the manufacturer's protocols (Elabscience Biotechnology, #E-BC-K006-M). All samples were tested three times, and the absorbance was measured at 450 nm with a Microplate Reader (Thermo).

2.13. Western blot

The total protein of the pancreatic tissues was extracted using a RIPA lysate containing protease inhibitor and phosphatase inhibitor, and protein concentrations were measured according to the manufacturer's manual. Subsequently, the protein was separated by the sodium dodecyl sulfate-polyacrylamide gel electrophoresis and transferred to nitrocellulose membrane. After being sealed with 5% skim milk, incubation with primary antibody overnight at 4 °C, and then incubation with the secondary antibody. Finally, Tanon 5500 Chemiluminescent Imaging System (Tanon, Shanghai, China) was used to develop protein bands. The primary antibodies involved in this experiment included anti-p-p65 (CST,

#3033), anti-p65 (CST, #8242), anti-p-I κ B α (CST, #2859P), anti-I κ B α (CST, #4814) and anti- β -actin (Proteintech, HRP-60008).

2.14. Real-time PCR

Total RNA was extracted from mouse pancreas tissues using the TRIzol reagent (Invitrogen). The cDNA was synthesized according to the manufacturer's protocol using a Reverse Transcription Kit (TaKaRa, #RR036A). PCR amplification of individual mRNAs using SYBR Green PCR Master Mix (TaKaRa, #RR820A) detection as described in the manufacturer's manual. The primers used for this experiment are listed in Supporting Information Table S3 and the data were analyzed using the $\Delta\Delta C_t$ method.

2.15. Statistical analysis

All data were expressed as mean \pm standard deviation (mean \pm SD), and were analyzed using GraphPad Prism 8. One-way ANOVA was used for comparison between multiple groups, and *t*-test was used for comparison between two groups. *P* < 0.05 was considered statistically significant.

3. Results

3.1. The development of anti-human PSGL-1-specific monoclonal antibodies

A sequential administration of DNA and a novel K562 cell-based vaccine with confirmed expression of human PSGL-1 (Supporting Information Fig. S1), followed by a boost with recombinant fusion protein of extracellular domain of human PSGL-1 and Fc fragment of human IgG2 (PSGL-1-ECD-Fc) in *Rhesus macaques* (*Macaca mulatta*). Blood samples (10 mL per subject) were collected from rhesus macaques on Day 14 post boosting with the PSGL-1-ECD-Fc vaccine and peripheral blood mononuclear cells (PMBCs) were freshly isolated (Fig. 1A). To develop a gating strategy for isolation of macaque antibody secreting cells from PMBCs, antibodies for a panel of surface markers (CD3, CD14, CD20, CD27, IgG) were selected based on the NHP database (<http://www.nhpagents.org>). Activated/memory B cells with CD3⁺/CD14⁻/CD20⁺/CD27⁺/IgG⁺ were sorted into 96-well plates for four cells per well for subsequent antibody genes cloning (Fig. 1B). Cells were then stimulated for differentiation into plasma cells to produce IgG by culturing with CD40L-expressing feeder cells and IL-2, as well as IL-21. To screen the candidate antibody, the cell culture supernatant was determined using PSGL-1 (ECD)-specific ELISA assay (Supporting Information Fig. S2) and 1C6, 2C12, 2D6, 2D12, 2E2, 2F2, 2H1, 3F4, 3G6 and 3H2 wells were identified with high binding affinity than blank control (Fig. 1C). Then genes encoding Ig VH, Ig VK and V λ from positive wells were recovered by PCR (Fig. 1D), cloned into human IgG heavy- and light-chains expression vectors and expressed by transfection of HEK293T cells. All combinations of heavy- and light-chains obtained from a well must be paired and expressed to regenerate the natural heavy- and light-chains pairs and determine their binding activity. The results show that two monoclonal antibodies (mAbs), named RH001-6 and RH001-22, could specifically bind to PSGL-1, which were recovered from wells of 2H1 and 3H2, respectively. The binding kinetics of PSGL-1 (ECD) for these two mAbs were measured by Surface

Plasmon Resonance (SPR) using Pro A chip. The K_D values of antibodies RH001-6 and RH001-22 for full purified human PSGL-1 expressed in HEK293 cells measured *via* SPR are 1.61E-08 mol/L (16.1 nmol/L) and 5.53E-08 mol/L (55.3 nmol/L), respectively (Fig. 1E and Supporting Information Fig. S3), which were further corroborated by CM5 chip (Fig. 1F). Interestingly, we identified a near 45-fold decrease for the cross affinity of RH001-6 antibody to mouse PSGL-1 (9.27E-07 mol/L, 927 nmol/L) when compared with its affinity to human PSGL-1 (2.06E-08 mol/L, 20.6 nmol/L) through Series Sensor chip CM5 measurement (Fig. 1F and Supporting Information Fig. S4A and S4B). Furthermore, ELISA binding experiment showed that the cross-reactive affinity of RH001-6 was higher than that of the anti-human PSGL-1 antibody KPL1, though lower than that of anti-mouse PSGL-1 antibody 4RA10 (Fig. S4C). In addition, we also used the IgBLAST tool to analyze the homology between RH001-6 and RH001-22 variable regions and humans, and found that RH001-6-VK has 84%–88% homology, RH001-6-VH has 90%–93% homology (Table 1).

3.2. RH001-6 efficiently blocks the binding of PSGL-1 to P-selectin on endothelial cells

To verify the specificity of RH001-6 and RH001-22 to bind to PSGL-1 *in vitro*, we firstly used flow cytometry to examine the ability of RH001-6 and RH001-22 to block the binding of P-selectin to peripheral blood mononuclear cells (THP-1 cells). Fluorescence labeled recombinant human P-selectin (CD62P-Fc) chimera proteins were incubated with THP-1 cells in the presence of RH001-6 and RH001-22 antibodies or isotype control antibody (IgG1) for 30 min, and then the percentage of recombinant human P-selectin positive THP-1 cells were quantified using flow cytometry. As shown in Fig. 2A and B, RH001-6 and RH001-22 treatments reduced P-selectin positive THP-1 cells in a dose-dependent manner. To determine whether RH001-6 and RH001-22 could functionally block the interaction of lymphocytes and endothelial cells, we co-incubated green 5-chloromethylformatin diacetate (CMFDA) stained THP-1 cells and human umbilical vein endothelial cells (HUVECs) to determine the adhesion ability of leukocytes to endothelial cells in the presence of RH001-6, RH001-22 or IgG1. The results show that RH001-6 and RH001-22 significantly reduced the adhesion between THP-1 cells and endothelial cells, and the inhibition rate of RH001-6 increased in a dose-dependent manner (Fig. 2C and D). These results suggest that both RH001-6 and RH001-22 could interrupt the adhesion of lymphocytes to endothelial cells by blocking the binding of PSGL-1 to P-selectin, and RH001-6 is more efficient than RH001-22 in blocking adhesion. Therefore, we will mainly verify the function of RH001-6.

In vitro, we compared the effect of RH001-6 to other available anti-PSGL-1 antibodies, KPL1 and 4RA10 on the binding of P-selectin to PSGL-1. The results show that in the presence of RH001-6 and KPL1, the number of THP-1 cells binding to P-selectin positive endothelial cells significantly decreased, and the blocking effect of RH001-6 was profoundly higher than that of KPL1 (Supporting Information Fig. S5A and S5B). As expected, 4RA10 show only minimal effect on the adhesion of leukocytes to endothelial cells since 4RA10 is specific to bind to mouse PSGL-1 (Fig. S5). These results demonstrate that RH001-6 is highly effective on interrupting the interaction between PSGL-1 and P-selectin *in vitro*.

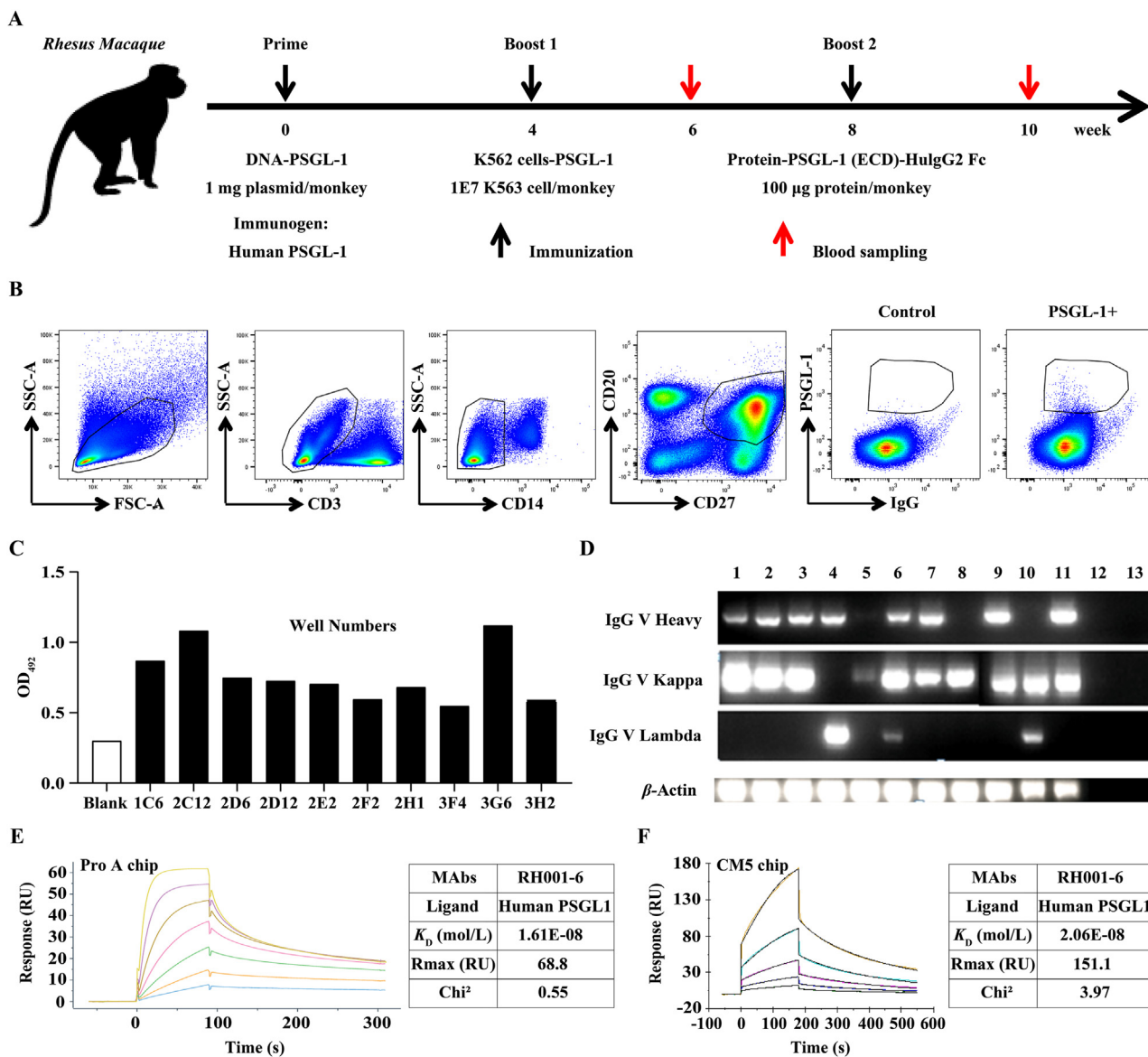


Figure 1 Sorting of antibody secreting cells and cloning of IG variable domain genes from antibody secreting cells. (A) Schematic illustration of immunization and blood sampling schedule, and animal group information. (B) Sorting results of peripheral blood mononuclear cells (PBMCs) are isolated 2 weeks after the second boost. Sorting results are shown in the contour graphs. (C) ELISA reactivity of cell culture supernatants after 13 days to recombinant PSGL-1 (ECD) protein. (D) Representative gel picture showing polymerase chain reaction (PCR) products of VH, V-KAPPA or V-LAMBDA domain genes and β -actin amplified from antibody secreting cells. (E, F) The surface plasmon resonance (SPR) traces show binding curves and SPR-based kinetic affinity of RH001-6 to human PSGL-1 protein using Pro A chip (E) and CM5 chip (F) detection.

3.3. RH001-6 treatment relieves tissue damages and inflammatory responses in caerulein-induced acute pancreatitis mice

The tethering and rolling of leukocytes in acute inflammatory responses are mainly mediated by the interaction between PSGL-1 and P-selectin, and interrupting this interaction has become an interesting pharmacological target for the treatment of acute inflammatory responses. Our results above have proved that anti-PSGL-1 mAb RH001-6 can effectively abolish the adhesion of leukocytes and endothelial cells by blocking the interaction between PSGL-1 and P-selectin, we next explored whether RH001-6 can treat acute pancreatitis (AP) *in vivo*.

Firstly, we examined the efficacy of systemic injections of RH001-6 in caerulein plus lipopolysaccharide (LPS) induced AP model using male BALB/c nude mice. Caerulein plus LPS induced severe destruction of the pancreatic tissue structure, characterized as edema, leukocyte infiltration, and extensive acinar cell necrosis in the pancreas (Fig. 3A). In contrast, these pathological changes were alleviated both in 10 mg/kg RH001-6 and 4RA10 treatment groups. More strikingly, the pancreatic tissue structures of the mice treated with 10 mg/kg RH001-6 almost remained intact, and the interstitial edema, acinar cell necrosis and inflammatory cells infiltration of the pancreas were significantly reduced (Fig. 3A). Compared with 4RA10, RH001-6 also effectively alleviated AP-associated pancreatic damage, which were

Table 1 Homology analysis of RH001-6 and RH001-22 variable region with human using IgBlast tool.

Variable region	From	to	Length	Matches	Mismatches	Gaps	Identity (%)
Alignment summary between RH001-6 VH and top germline V gene hit							
FR1-IMGT	1	25	25	22	3	0	88
CDR1-IMGT	26	34	10	8	1	1	80
FR2-IMGT	35	51	17	16	1	0	94.1
CDR2-IMGT	52	59	8	5	2	1	62.5
FR3-IMGT	60	97	38	37	1	0	97.4
CDR3-IMGT (germline)	98	99	2	1	1	0	50
Total			100	89	9	2	89
Alignment summary between RH001-6 VL and top germline V gene hit							
FR1-IMGT	1	26	26	23	3	0	88.5
CDR1-IMGT	27	37	11	10	1	0	90.9
FR2-IMGT	38	54	17	14	3	0	82.4
CDR2-IMGT	55	57	3	2	1	0	66.7
FR3-IMGT	58	93	36	35	1	0	97.2
CDR3-IMGT (germline)	94	100	7	4	3	0	57.1
Total			100	88	12	0	88
Alignment summary between RH001-22 VH and top germline V gene hit							
FR1-IMGT	1	25	25	23	2	0	92
CDR1-IMGT	26	33	8	6	2	0	75
FR2-IMGT	34	50	17	14	3	0	82.4
CDR2-IMGT	51	58	8	3	4	1	37.5
FR3-IMGT	59	96	38	30	8	0	78.9
CDR3-IMGT (germline)	97	98	2	1	1	0	50
Total			98	77	20	1	78.6
Alignment summary between RH001-22 VL and top germline V gene hit							
FR1-IMGT	4	25	22	17	5	0	77.3
CDR1-IMGT	26	33	8	5	3	0	62.5
FR2-IMGT	34	50	17	14	3	0	82.4
CDR2-IMGT	51	53	3	3	0	0	100
FR3-IMGT	54	89	36	31	5	0	86.1
CDR3-IMGT (germline)	90	98	9	5	4	0	55.6
Total			95	75	20	0	78.9

further corroborated by the histological score and plasma amylase levels (Fig. 3B and C). Furthermore, we identified that RH001-6 treatment markedly restrained the elevation of plasma IL-6, TNF- α and IFN- γ cytokines in mice induced by caerulein plus LPS, and this effect was equal to 4RA10 (Fig. 3D). We also confirmed that RH001-6 treatment suppressed IL-6, TNF- α , and IFN- γ response in the pancreatic tissues (Supporting Information Fig. S6). These data suggest that RH001-6 can significantly alleviate pancreatic injury by reducing inflammatory cytokines production induced by caerulein plus LPS *in vivo*.

In AP, damaged acinar cells release chemokines or cytokines and express various adhesion molecules, which recruit and mediate the infiltration of immune cells into the injured site^{31–33}. Once immune cells infiltrate the pancreas, the cellular contents released from necrotic and damaged cells activate monocytes and neutrophils which further fuel inflammation^{6,34}. To determine the effect of RH001-6 treatment on leukocyte infiltration in AP mice, we quantified the number of monocytes and neutrophils in peripheral blood and pancreatic tissues of AP mice induced by caerulein plus LPS. Flow cytometry analysis showed that 10 mg/kg RH001-6 treatment significantly decreased the proportion of monocytes (Ly6c positive cells, Ly6c⁺) and neutrophils (Ly6g positive cells, Ly6g⁺) in peripheral blood of mice (Fig. 3E). We also found that the administration of 10 mg/kg RH001-6 could reduce infiltration of neutrophils (myeloperoxidase, MPO) and macrophages (F4/80) in the pancreatic tissues (Fig. 3F). These results demonstrate that RH001-6 treatment leads to the reduction

of the infiltration of neutrophils and macrophages in the pancreatic tissues of AP mice and thereby attenuates the inflammatory responses.

3.4. RH001-6 treatment attenuates L-arginine-induced acute pancreatitis

To evaluate whether the protective effect of RH001-6 against pancreatitis is a general phenomenon rather than associated with the caerulein-specific mechanism, we used another AP model induced by L-arginine. Histologically, less tissue necrosis was observed in the pancreas from RH001-6 or 4RA10 treated mice compared with the pancreas from mice treated with isotype control antibody IgG1 (Fig. 4A). Furthermore, histological score revealed that the increase of acinar necrosis was significantly less prominent in the pancreas from RH001-6 or 4RA10 treated mice than IgG1 groups (Fig. 4B). Again, the increase in serum amylase in RH001-6 or 4RA10 groups during L-arginine induced AP were significantly less pronounced than IgG1 groups (Fig. 4C). Importantly, the inflammatory cytokines IL-6, TNF- α as well as IFN- γ all decreased in plasma and pancreas of RH001-6 or 4RA10 treated groups (Fig. 4D and Supporting Information Fig. S7). Moreover, similar to 4RA10, RH001-6 significantly reduced the percentage of monocytes (Ly6c⁺) and neutrophils (Ly6g⁺) in peripheral blood of mice, and reduced the infiltration of and neutrophils (MPO) and macrophages (F4/80) in the pancreatic tissues induced by L-arginine (Fig. 4E and F). These

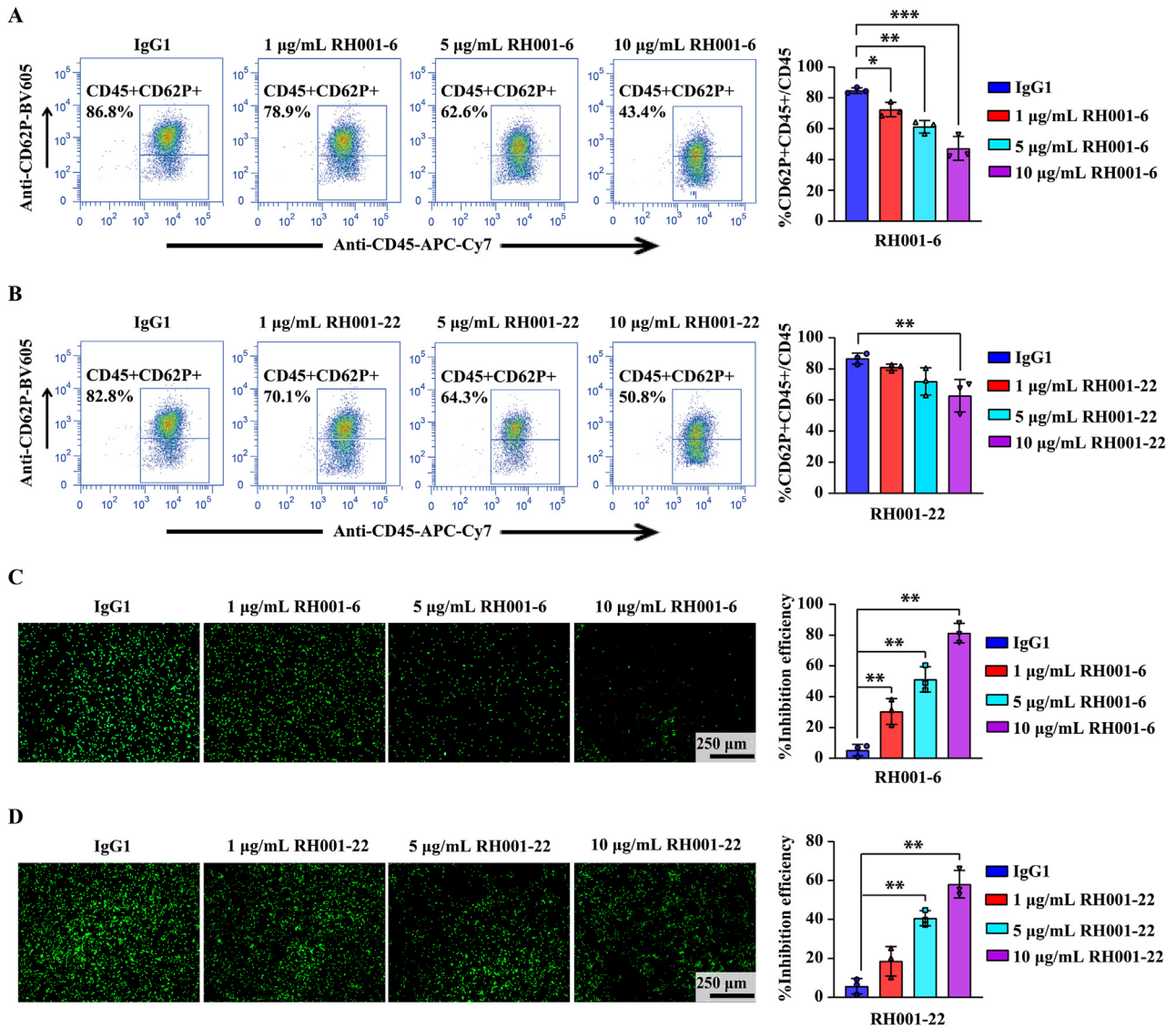


Figure 2 RH001-6 blocks the adhesion efficiency of leukocytes and endothelial cells. (A, B) Flow cytometry analysis of P-selectin⁺ (CD62P⁺) and peripheral blood monocytes (THP-1 cells, CD45⁺) after treatment with RH001-6 (A) or RH001-22 (B), and quantitative data of the percentage of CD62P⁺CD45⁺/Total CD45⁺ cells in different groups. (C, D) Representative photographs of adhesion between THP-1 cells treated with different concentrations RH001-6 (C) or RH001-22 (D) and human umbilical vein endothelial cells (HUVECs), and quantitative analysis of adhesion inhibition rate. Data are expressed as mean \pm SD, $n = 3$; * $P < 0.05$, ** $P < 0.01$, *** $P < 0.001$ vs. Control group.

results confirm that RH001-6 has protective effect in L-arginine induced AP model.

3.5. RH001-6 treatment inhibits NF- κ B pathway and gene expression of adhesion molecules in experimental acute pancreatitis mice

Transcription factor nuclear factor (NF)- κ B is activated in the early stage of pancreatitis and increases the expression of a variety of pro-inflammatory genes^{35–37}. In addition, the increase in NF- κ B activity in acinar cells is related to the severity of AP³⁷. Given the central role of this pathway in driving and aggravating the inflammatory response of AP, we examined the NF- κ B pathway in the pancreatic tissue of AP mice by Western blot and immunofluorescence staining. The results showed that RH001-6 treatment significantly reduced the phosphorylated protein levels of p65 and I κ B α in pancreas in two AP models induced by caerulein (Fig. 5A and B)

or L-arginine (Fig. 5C and D). Since PSGL-1 is mainly expressed in leukocytes, we performed immunofluorescent co-localization of p65 and neutrophils marker MPO or macrophages marker CD68, and found that the nuclear translocation of p65 observed in neutrophils and macrophages were inhibited by RH001-6 or 4RA10 treatment (Fig. 5E–H). Moreover, the mRNA levels of the adhesive molecules in the RH001-6 or 4RA10 groups were also down-regulated (Fig. 5I and J). These results suggest that RH001-6 treatment may be able to additionally suppress NF- κ B pathway to abolish the subsequent inflammatory responses in AP.

3.6. No systemic toxicity and side effects during the treatment of RH001-6

Next, we investigated whether the intravenous administration of RH001-6 could cause systemic toxicities and side effects in two different AP models. Organs including heart, liver, spleen, lung,

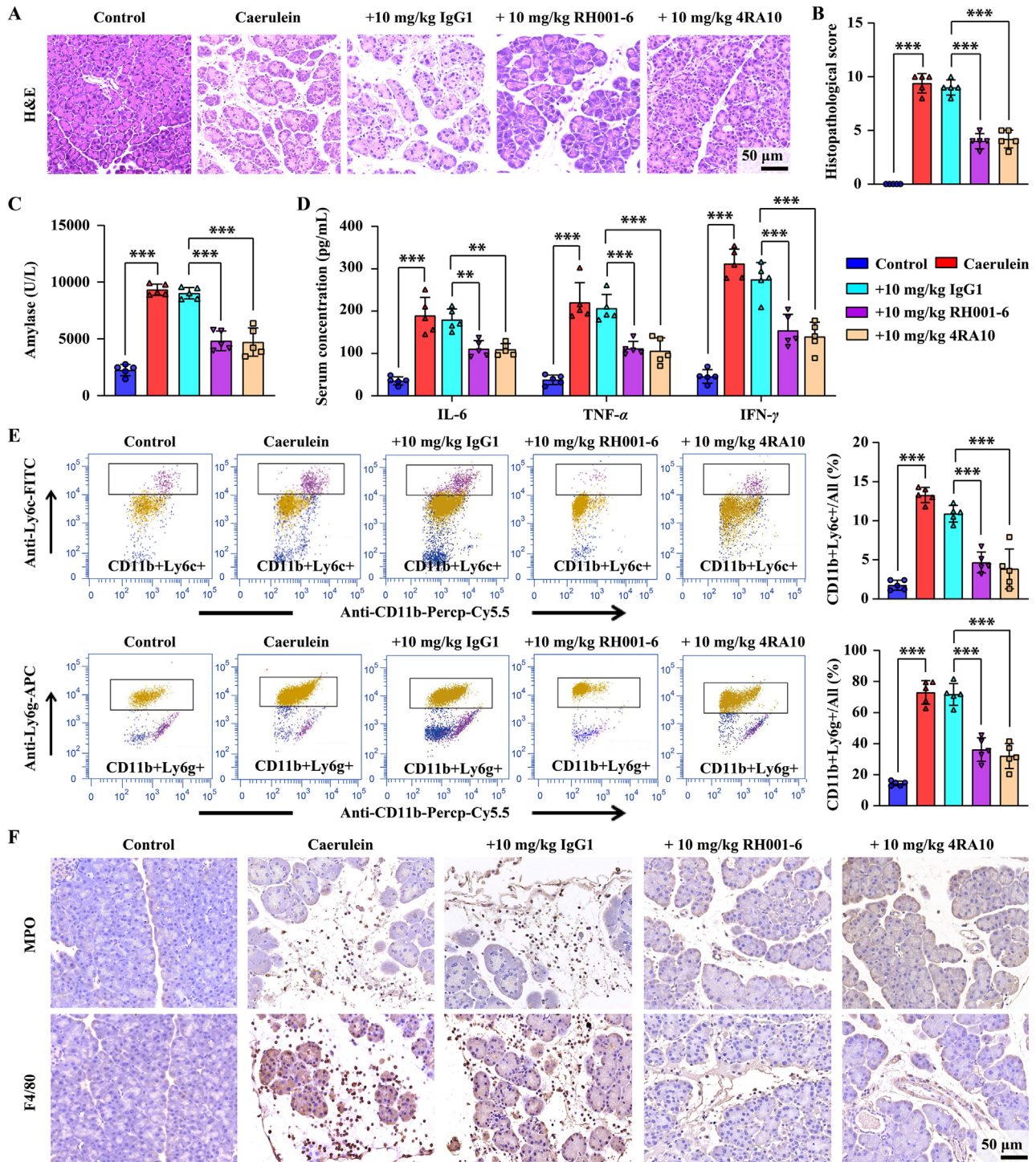


Figure 3 RH001-6 treatment alleviates pancreatic injury and inflammatory response in acute pancreatitis (AP) induced by caerulein. (A) H&E staining of pancreatic tissues in each group. (B) The histopathological score of the pancreases. (C) The amylase level of serum. (D) Serum inflammatory cytokines levels. (E) Flow cytometry and quantification for monocytes (Ly6c positive cells, Ly6c⁺) and neutrophils (Ly6g positive cells, Ly6g⁺) in peripheral blood. (F) Representative immunohistochemically images of neutrophils (MPO) and macrophages (F4/80) positive cells in caerulein-induced AP mouse pancreas. Data are expressed as mean ± SD, $n = 5$; *** $P < 0.001$ vs. Control group; ** $P < 0.01$, *** $P < 0.001$ vs. IgG1 group.

and kidney from different treatment groups were sectioned and stained with H&E. No abnormalities of histological structure were observed in all organs in the caerulein-induced AP model (Fig. 6A). Moreover, plasma evaluations reflecting liver damage

(ALT, AST, and TBIL levels), cardiac injury (CK levels) and renal damages (BUN and CRE levels) showed no significant differences between RH001-6 and IgG1 groups in caerulein-induced AP model (Fig. 6B). The same results were observed in the L-arginine

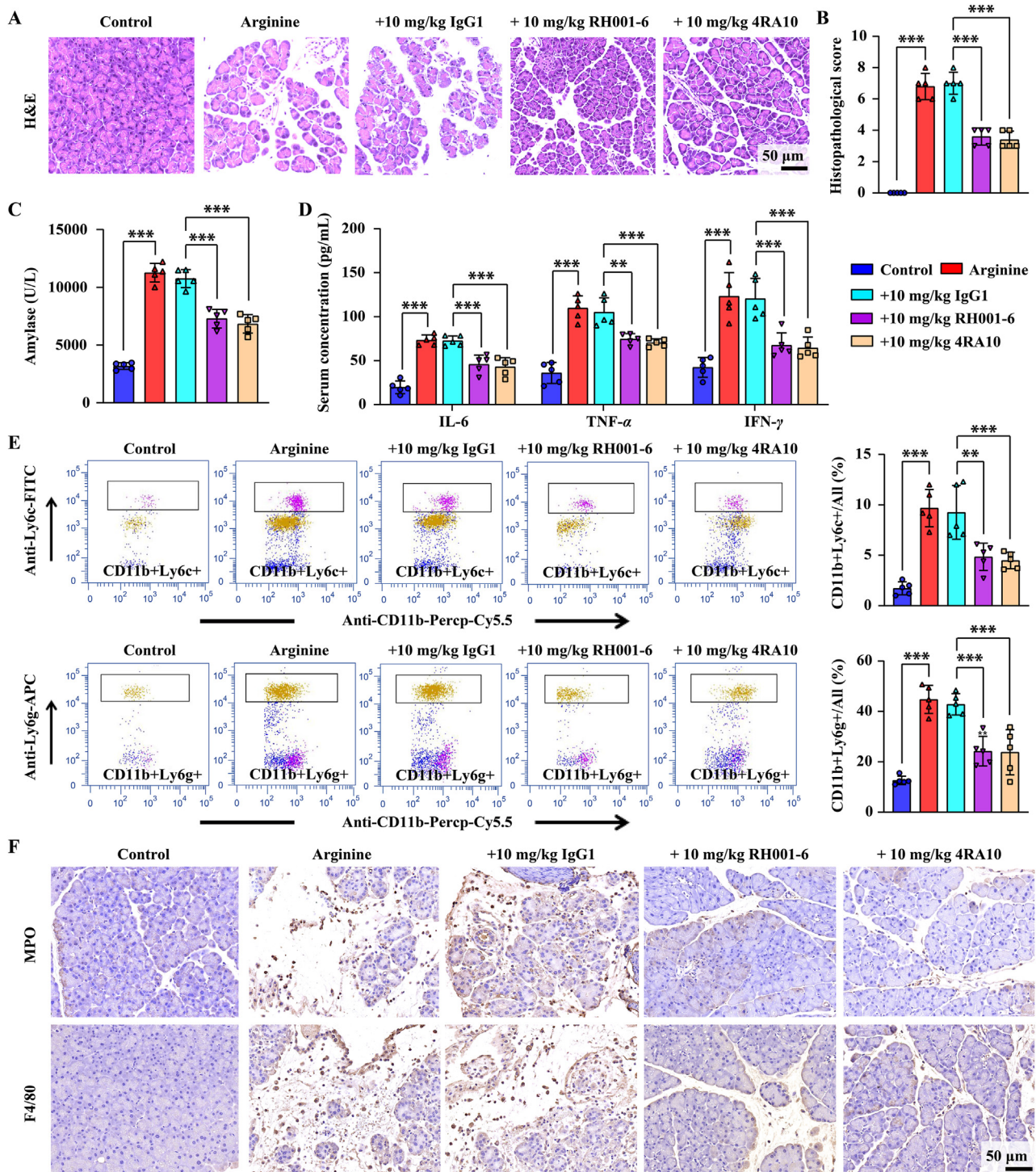


Figure 4 RH001-6 treatment alleviates pancreatic damage and inflammatory response in L-arginine- induced AP *in vivo*. (A) H&E staining of pancreatic tissues in each group. (B) The histopathological score of pancreases. (C) Serum amylase activity was measured by ELISA test. (D) Serum inflammatory cytokines levels. (E) Flow cytometry and quantification for monocytes (Ly6c⁺) and neutrophils (Ly6g⁺) in peripheral blood. (F) Representative immunohistochemically images of neutrophils (MPO) and macrophages (F4/80) positive cells in L-arginine induced AP mouse pancreas. Data are expressed as mean ± SD, $n = 5$, *** $P < 0.001$ vs. Control group; ** $P < 0.01$, *** $P < 0.001$ vs. IgG1 group.

induced AP model (Supporting Information Fig. S8). Altogether, these data show that the systemic administration of RH0016 is safe and does not cause any significant systemic toxicities and side effects.

4. Discussion

Acute pancreatitis (AP) is a global health issue with high morbidity and mortality, which is characterized by aseptic

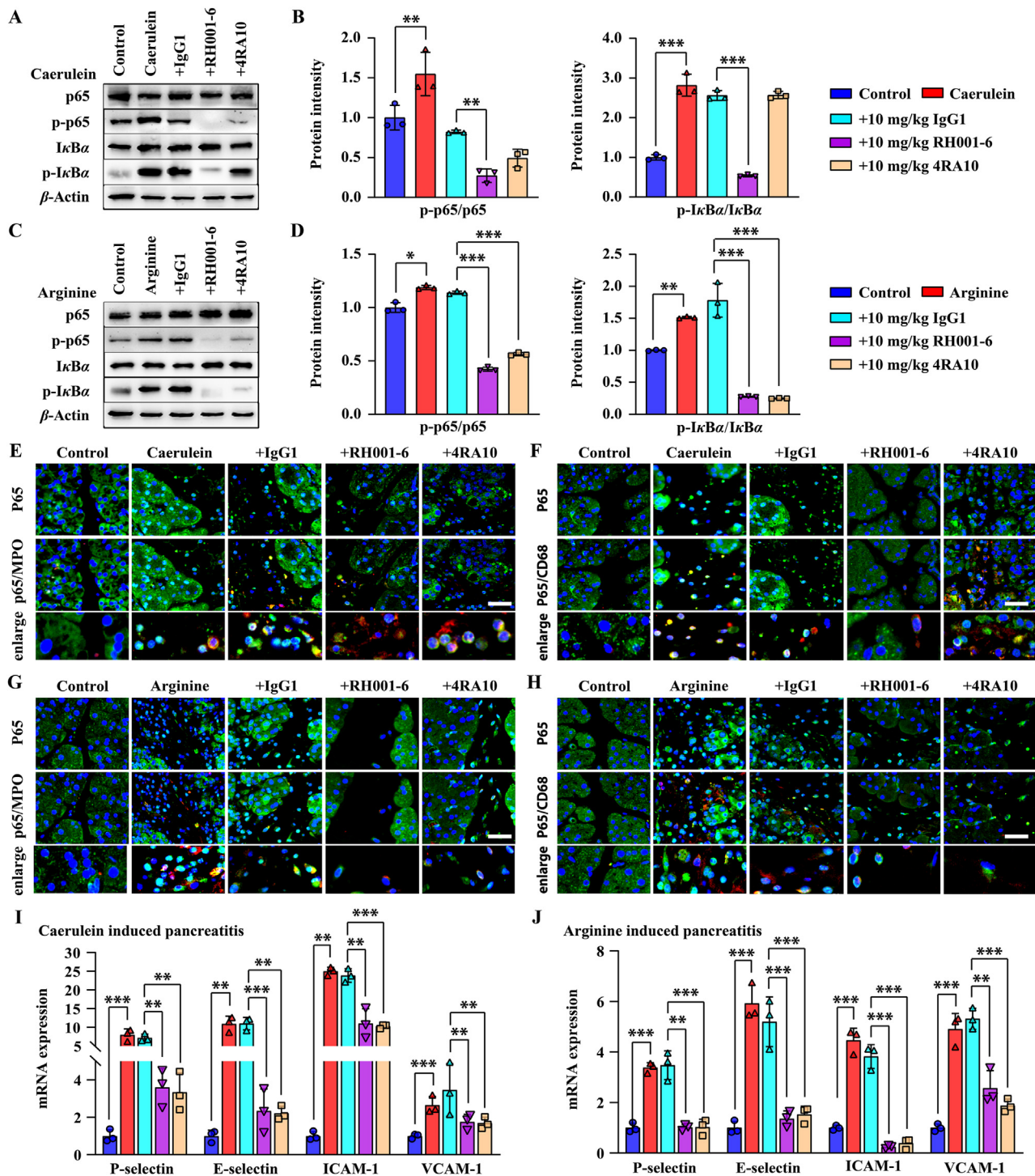


Figure 5 RH001-6 treatment inhibits the NF- κ B pathway and reduces adhesion molecule expression. (A–D) Protein expression and quantitative analysis of p-p65 and p-I κ B α in the pancreatic tissue of AP model induced by caerulein (A, B) and L-arginine (C, D). (E–G) Representative immunofluorescence images of p65/MPO (E) and p65/CD68 (F) in caerulein induced AP mouse pancreas, and p65/MPO (G) and p65/CD68 (H) in L-arginine-induced AP mouse pancreas. (I, J) The mRNA levels of adhesion molecules in caerulein- (I) and L-arginine- (J) induced AP mouse pancreas. Data are expressed as mean \pm SD, $n = 3$, * $P < 0.05$, ** $P < 0.01$, *** $P < 0.001$ vs. Control group; ** $P < 0.01$, *** $P < 0.001$ vs. IgG1 group.

inflammation of the pancreas. Despite extensive efforts in the past decades, there is still no available drug therapy to treat AP^{38–40}. It is well established that PSGL-1 plays a central role in inflammatory diseases, and we previously demonstrated that PSGL-1

deficiency prevents development of AP by attenuating leukocyte infiltration¹⁹, and accumulating evidence revealed the potent anti-inflammation effect of PSGL-1 blockade. Therefore, in this study we developed a non-human primate derived PSGL-1 antibody and

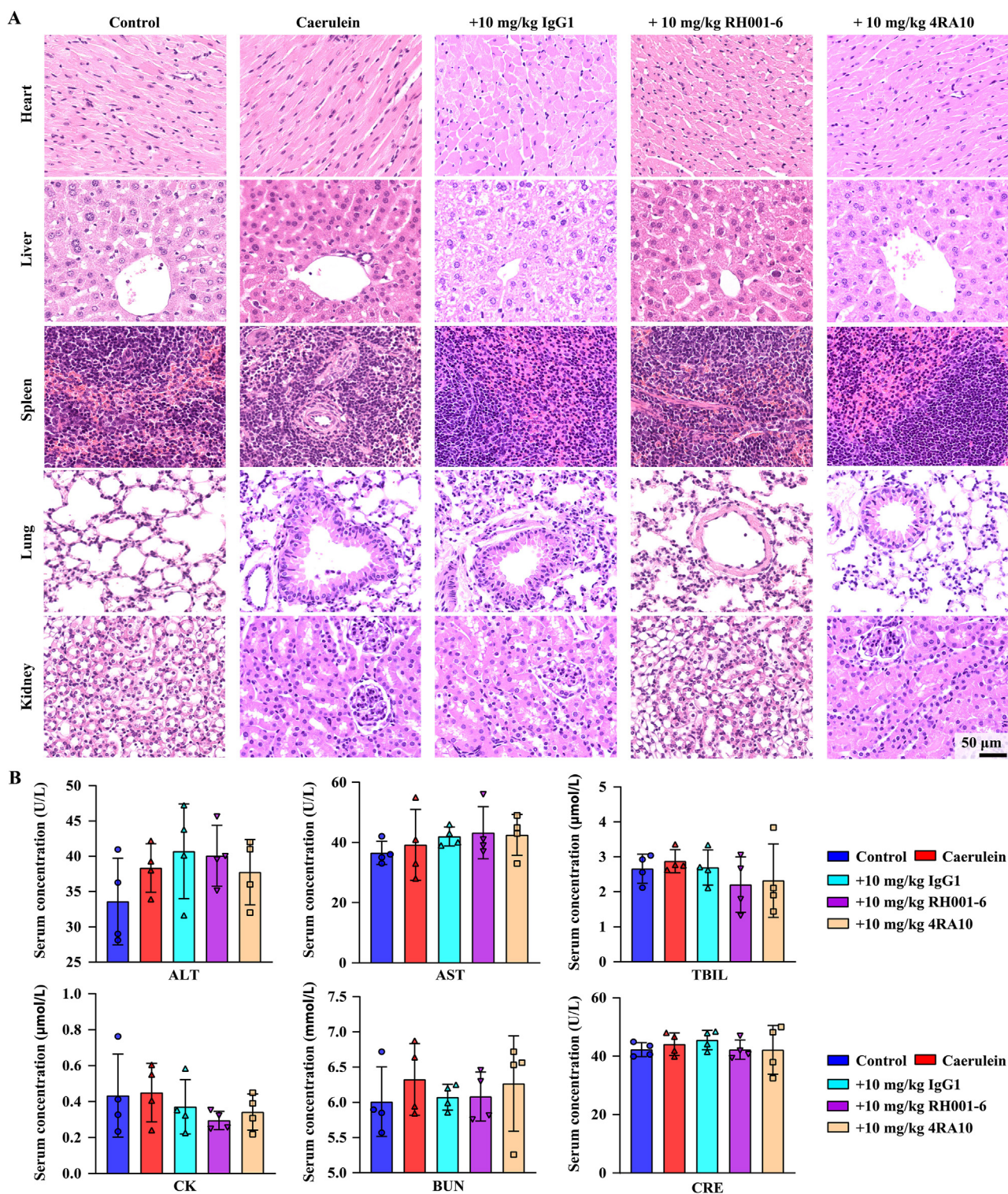


Figure 6 *In vivo* biosafety of RH001-6 treatment in AP model induced by caerulein. (A) Representative images of H&E staining of main organs in AP mice. (B) Plasma levels of alanine transaminase (ALT), aspartate transaminase (AST), total bilirubin (TBIL), creatine kinase (CK), blood urea nitrogen (BUN), and creatinine (CRE) in different groups. Data are expressed as mean \pm SD, $n = 4$.

evaluated its efficacy in treating AP. Here, we reported that anti-PSGL-1 monoclonal antibody (mAb) RH001-6 confer effective protection on diseases-associated inflammation and tissue damage in mouse models of both caerulein- and L-arginine-induced AP,

which is related to NF- κ B inhibition (Fig. 7). Most of important, RH001-6 had no treatment-related toxic effects on other organs. To the best of our knowledge, this is the first study to report the role of anti-PSGL-1 mAb in AP, which provides a novel

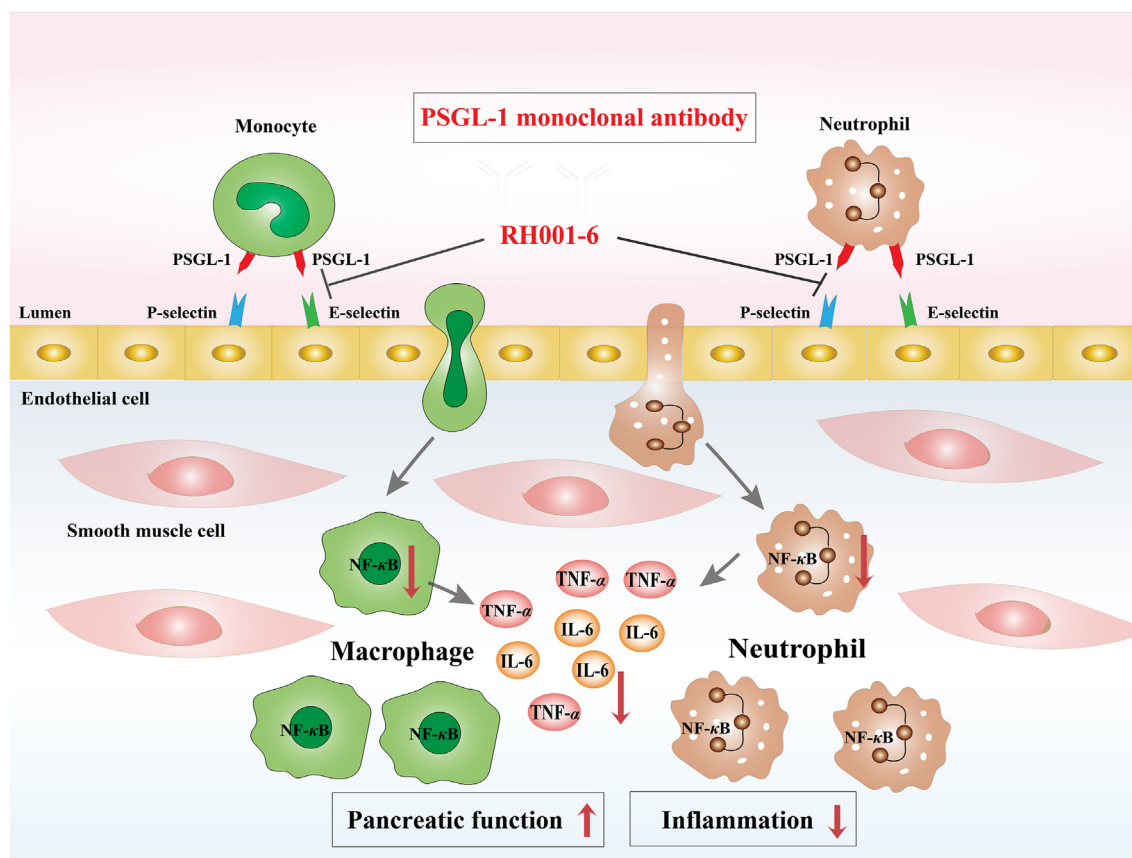


Figure 7 The illustrated mechanism of PSGL-1 monoclonal antibody (RH001-6) in the treatment of inflammatory diseases.

therapeutic option for AP treatment, and has important clinical significance and transformation value not only for AP but also for other inflammatory diseases.

As a cell surface adhesion molecule, PSGL-1 is expressed in neutrophils, natural killer cells, monocytes, dendritic cells, T and B lymphocytes, and some CD34⁺ stem cells. It is also abundant on the surface of platelets in the early stage of differentiation^{41–46}. The expression of PSGL-1 increases rapidly under inflammatory conditions, which induces leukocyte rolling and tethering on vascular endothelial cells by binding with P-, E-, and L-selectins on the surface of vascular endothelial cells, followed by transmigration of the leukocytes into tissues^{21,47,48}. Currently, extensive studies have documented the beneficial effect of PSGL-1 blockade in different inflammatory settings using experimental animal models^{15,21,49}. Although a previous study has demonstrated that anti-PSGL-1 antibody decreased caerulein-induced leukocyte rolling, hardly any indicators related to disease phenotype were observed in this study⁵⁰. Because PSGL-1 mediates the pathological recruitment of leukocytes at the site of inflammation, PSGL-1 antibody or inhibitor has become a potential candidate for anti-inflammatory drugs. Several PSGL-1 monoclonal antibodies (mAbs) are in the clinical trial stage now, such as, Neihulizuma [[ClinicalTrials.gov](https://clinicaltrials.gov/ct2/show/study/NCT03298022) Identifier: NCT03298022], selk2 and so on. However, no clinical trial implied the role of PSGL-1 mAbs in AP and no mAbs targeting PSGL-1 are available clinically so far. Therefore, it is important to elucidate the role of PSGL-1 mAbs in the treatment of AP⁵¹.

The development of PSGL-1 antibody currently mainly comes from mouse sources, and the whole human antibody of PSGL-1

has not been used. As known, rhesus macaque derived antibody shares >95% homogeneous sequences with human antibody⁵². Therefore, strategy to develop antibody drug from rhesus macaques represents a preferential alternative to human antibody, particular in the case of failure directly generating antibody from human B-cell receptor (BCR) profile. There are other advantages to employ the primate monkey to generate antibodies against human derived antigens. For example, the vaccination in primate monkey with human derived antigen could ensure to generate antigen specific antibodies and gain druggable antibodies. In this study, we developed two non-human primate derived mAbs against human PSGL-1 (RH001-6 and RH001-22) from human PSGL-1 as immunogen immunized rhesus macaques. We demonstrate that 1) RH001-6 and RH001-22 bound to both human PSGL-1 ligand and mouse PSGL-1 ligand, with higher affinity to the former, 2) RH001-6 and RH001-22 inhibited the binding of P-selectin to THP-1 cells and the adhesion of THP-1 cells to endothelial cells in a concentration-dependent manner. Interestingly, the blocking effect of RH001-6 on PSGL-1 is superior than RH001-22 at the same concentration, which may be due to the higher binding affinity of RH001-6 to PSGL-1. Moreover, the blocking effect of RH001-6 on PSGL-1 was equal to another available anti-PSGL-1 antibody KPL1, highlighting the effectiveness of RH001-6.

To clarify the effect of anti-PSGL-1 mAb in AP, we performed *in vivo* experiments using two different experimental AP models to prevent model-specific effects, including caerulein- and L-arginine-induced AP mice. Our results proved that in both AP models, the administration of RH001-6 effectively relieved the

severity of AP, as evidenced by a remarkable decrease of serum amylase, obvious amelioration of pathological damage of murine pancreas, substantial reduction of inflammatory cytokines and less infiltration of neutrophils and macrophages in the pancreas. At the same time, we also detected the effect of anti-mouse PSGL-1 antibody 4RA10 in treating AP. 4RA10 has been demonstrated to decrease caerulein-induced leukocyte rolling⁵⁰, and inhibit neointima formation in atherosclerosis⁴⁹. We found that 4RA10 was similarly effective in decreasing inflammatory response and ameliorating pancreatic damage, highlighting the beneficial effect of PSGL-1 blockade in AP. As to the underlying mechanism, we focused on NF- κ B signaling pathway⁵³. As reported, NF- κ B pathway is activated in the development of AP^{54–56}, and PSGL-1 deficiency is related to inhibited activation of NF- κ B⁵⁷. Thus, we wondered whether NF- κ B signaling pathway is involved in the amelioration of inflammatory response and pancreatic damage of AP by RH001-6. As expected, the phosphorylation of I κ B α and p65 in the pancreatic tissue were significantly decreased after RH001-6 treatment. Moreover, we found that nuclear translocation of p65 could be observed in neutrophils and macrophages, which probably is responsible for the subsequent changes of inflammatory cytokines and adhesion molecules.

Of note, we found that RH001-6 was well tolerated and no treatment-related toxic effects were observed, which further increases the possibility of success for subsequent clinical trials. Unlike viral delivery of PSGL-1 siRNA or genetic deletion methods, intravenous injection of RH001-6 is clinically viable strategy, especially considering that it is completely human in sequence, which minimizes the risk of immunogenicity in patients, but further studies should be conducted to test the immunogenicity of RH001-6 in good laboratory practice (GLP) and investigational new drug (IND)-enabling pharmacology⁵⁸.

However, there are some limitations for our study. Firstly, we chose mice to verify the effect of RH001-6. Further experiments using monkey model and humanized PSGL-1 mouse model will be required for harnessing the full potential of anti-PSGL-1-mediated anti-inflammation therapy in more inflammatory diseases including AP. Secondly, we found that RH001-6 not only reduced the neutrophils and macrophages infiltration in pancreas, but also decreased peripheral monocytes and neutrophils counts, different with the study by Rijcken EM et al.²¹. The discrepancy in the results may be explained by different PSGL-1 mAbs and different administration routes. The reduced peripheral monocytes and neutrophils counts by antibody blockade of PSGL-1 implies that PSGL-1 may play a critical role in hematopoiesis, in view of the dynamic expression of functional PSGL-1 on bone marrow progenitors⁵⁹. Thirdly, our results demonstrated that RH001-6 could bind to both human PSGL-1 and mouse PSGL-1, but the recognition epitope within PSGL-1 that can be recognized by RH001-6 is unclear. It will be interesting to determine the recognition epitope by RH001-6, which will be helpful to identify synergistic antibody and further optimize the treatment regimen.

5. Conclusions

Anti-PSGL-1 mAb RH001-6 can ameliorate the severity of AP by attenuating inflammatory response. RH001-6 represents a promising candidate drug for the antibody-based treatment of inflammatory diseases, which provides a novel therapeutic strategy not only for AP, but also for a broad spectrum of other acute and chronic inflammatory diseases, including atherosclerosis,

hypertension, and abdominal aortic aneurysm, calling for additional research into the therapeutic potential of RH001-6 in those diseases.

Acknowledgments

This study was supported by Chinese Academy of Medical Sciences Innovation Fund for Medical Sciences (CAMS, 2021-I2M-1-072, China), National Natural Science Foundation of China (82161138027 and 81970358).

Author contributions

Jianqing Xu and Zhiwei Yang conceived and supervised the study. Yuhan Li, Xiangqing Ding, and Xianxian Wu designed and implemented experiments, analyzed data, and wrote charts and manuscripts. Xiangqing Ding and Longfei Ding designed, developed and identified the mono-clonal antibody. Yuhan Li, Yuhui Yang, Xiaoliang jiang, Xu zhang and Xing liu constructed the mouse model, injection, tissue collection and data analysis. Yuhan Li, Xioianxian Wu and Yuhui Yang contributed to cell experiment, immunoblotting, and immunohistochemistry and data analysis. Jianrong su, Jianqing Xu and Zhiwei Yang made critical revisions to the manuscript. And all authors reviewed and approved the manuscript.

Conflicts of interest

Yuhan Li, Jianqing Xu, Xiangqing Ding and Yuhui Yang are co-inventors on patent number 2021109591435 entitled “Antibodies Targeting PSGL-1 Protein and their Applications”. The other authors declare no competing interests.

Appendix A. Supporting information

Supporting data to this article can be found online at <https://doi.org/10.1016/j.apsb.2023.07.028>.

References

- Matta B, Gougol A, Gao X, Reddy N, Talukdar R, Kochhar R, et al. Worldwide variations in demographics, management, and outcomes of acute pancreatitis. *Clin Gastroenterol Hepatol* 2020;**18**:1567–75.
- Boxhoorn Lotte, Voermans Rogier P, Bouwense Stefan A, Bruno Marco J, Verdonk Robert C, Boermeester Marja A, et al. Acute pancreatitis. *Lancet* 2020;**396**:726–34.
- Krishna SG, Kamboj AK, Hart PA, Hinton A, Conwell DL. The changing epidemiology of acute pancreatitis hospitalizations: a decade of trends and the impact of chronic pancreatitis. *Pancreas* 2017;**46**:482–8.
- Windsor JA. Pancreatic enzyme replacement therapy in chronic pancreatitis: a long way to go. *Gut* 2017;**66**:1354–5.
- Song Y, Zhang Z, Yu Z, Xia G, Wang Y, Wang L, et al. Wip1 aggravates the caerulein-induced cell autophagy and inflammatory injury by targeting STING/TBK1/IRF3 in acute pancreatitis. *Inflammation* 2021;**44**:1175–83.
- Gukovskaya AS, Gukovsky I, Algul H, Habtezion A. Autophagy, inflammation, and immune dysfunction in the pathogenesis of pancreatitis. *Gastroenterology* 2017;**153**:1212–26.
- Kwon S, Kurmashev A, Lee MS, Kang JH. An inflammatory vascular endothelium-mimicking microfluidic device to enable I eukocyte

- rolling and adhesion for rapid infection diagnosis. *Biosens Bioelectron* 2020;**168**:112558.
8. Mehta P, Cummings RD, McEver RP. Affinity and kinetic analysis of P-selectin binding to P-selectin glycoprotein ligand-1. *J Biol Chem* 1998;**273**:32506–13.
 9. Goetz DJ, Greif DM, Ding H, Camphausen RT, Howes S, Comess KM, et al. Isolated P-selectin glycoprotein ligand-1 dynamic adhesion to P- and E-selectin. *J Cell Biol* 1997;**137**:509–19.
 10. Constantin G. PSGL-1 as a novel therapeutic target. *Drug News Perspect* 2004;**17**:579–86.
 11. Tinoco R, Otero DC, Takahashi AA, Bradley LM. PSGL-1: a new player in the immune checkpoint landscape. *Trends Immunol* 2017;**38**:323–35.
 12. Wang XL, Deng HF, Tan CY, Xiao ZH, Liu MD, Liu K, et al. The role of PSGL-1 in pathogenesis of systemic inflammatory response and coagulopathy in endotoxemic mice. *Thromb Res* 2019;**182**:56–63.
 13. Patel MS, Miranda D, Nieves, Chen J, Haller CA, Chaikof EL. Targeting P-selectin glycoprotein ligand-1/P-selectin interactions as a novel therapy for metabolic syndrome. *Transl Res* 2017;**183**:1–13.
 14. Kitamura K, Sato K, Sawabe M, Yoshida M, Hagiwara N. P-Selectin glycoprotein ligand-1 (PSGL-1) expressing CD4 T cells contribute plaque instability in acute coronary syndrome. *Circ J* 2018;**82**:2128–35.
 15. Wang Q, Wang H, Wang J, Venugopal J, Kleiman K, Guo C, et al. Angiotensin II-induced hypertension is reduced by deficiency of P-selectin glycoprotein ligand-1. *Sci Rep* 2018;**8**:3223.
 16. Wu X, Liu X, Yang H, Chen Q, Zhang N, Li Y, et al. P-selectin glycoprotein ligand-1 deficiency protects against aortic aneurysm formation induced by DOCA plus salt. *Cardiovasc Drugs Ther* 2022;**36**:31–44.
 17. Kappelmayer J, Nagy B. The interaction of selectins and PSGL-1 as a key component in thrombus formation and cancer progression. *Bio-Med Res Int* 2017;**2017**:6138145.
 18. Yang Y, Liu X, Liu Y, Fu H, Gao Y, Liu X, et al. The development of salt-sensitive hypertension regulated by PSGL-1 gene in mice. *Cell Biosci* 2018;**8**:20.
 19. Zhang X, Zhu M, Jiang XL, Liu X, Liu X, Liu P, et al. P-selectin glycoprotein ligand 1 deficiency prevents development of acute pancreatitis by attenuating leukocyte infiltration. *World J Gastroenterol* 2020;**26**:6361–77.
 20. Snapp KR, Ding H, Atkins K, Warnke R, Lusinskas FW, Kansas GS. A novel P-selectin glycoprotein ligand-1 monoclonal antibody recognizes an epitope within the tyrosine sulfate motif of human PSGL-1 and blocks recognition of both P- and L-selectin. *Blood* 1998;**91**:154–64.
 21. Rijcken EM, Laukoetter MG, Anthoni C, Meier S, Mennigen R, Spiegel HU, et al. Immunoblockade of PSGL-1 attenuates established experimental murine colitis by reduction of leukocyte rolling. *Am J Physiol Gastrointest Liver Physiol* 2004;**287**:G115–24.
 22. Muz B, Azab F, Puente P de la, Rollins S, Alvarez R, Kawar Z, et al. Inhibition of P-selectin and PSGL-1 using humanized monoclonal antibodies increases the sensitivity of multiple myeloma cells to bortezomib. *BioMed Res Int* 2015;**2015**:417586.
 23. Li J, Zhou Z, Zhang X, Zheng L, He D, Ye Y, et al. Inflammatory molecule, PSGL-1, deficiency activates macrophages to promote colorectal cancer growth through NFkappaB signaling. *Mol Cancer Res* 2017;**15**:467–77.
 24. He X, Ding L, Cao K, Peng H, Gu C, Li Y, et al. A human cell-based SARS-CoV-2 vaccine elicits potent neutralizing antibody responses and protects mice from SARS-CoV-2 challenge. *Emerg Microb Infect* 2021;**10**:1555–73.
 25. Huang J, Doria-Rose NA, Longo NS, Laub L, Lin CL, Turk E, et al. Isolation of human monoclonal antibodies from peripheral blood B cells. *Nat Protoc* 2013;**8**:1907–15.
 26. Meng W, Li L, Xiong W, Fan X, Deng H, Bett AJ, et al. Efficient generation of monoclonal antibodies from single rhesus macaque antibody secreting cells. *mAbs* 2015;**7**:707–18.
 27. Thatte A, Ficarro S, Snapp KR, Wild MK, Vestweber D, Hunt DF, et al. Binding of function-blocking mAbs to mouse and human P-selectin glycoprotein ligand-1 peptides with and without tyrosine sulfation. *J Leukoc Biol* 2002;**72**:470–7.
 28. Frenette PS, Denis CV, Weiss L, Jurk K, Subbarao S, Kehrel B, et al. P-selectin glycoprotein ligand 1 (PSGL-1) is expressed on platelets and can mediate platelet-endothelial interactions *in vivo*. *J Exp Med* 2000;**191**:1413–22.
 29. Dawra R, Sharif R, Phillips P, Dudeja V, Dhau lakhandi D, Saluja AK. Development of a new mouse model of acute pancreatitis induced by administration of L-arginine. *Am J Physiol Gastrointest Liver Physiol* 2007;**292**:G1009–18.
 30. Fu Q, Zhai Z, Wang Y, Xu L, Jia P, Xia P, et al. NLRP3 deficiency alleviates severe acute pancreatitis and pancreatitis-associated lung injury in a mouse model. *BioMed Res Int* 2018;**28**:1294951.
 31. Criddle DN, McLaughlin E, Murphy JA, Petersen OH, Sutton R. The pancreas misled: signals to pancreatitis. *Pancreatol* 2007;**7**:436–46.
 32. Jakkampudi A, Jangala R, Reddy BR, Mitnala S, Nageshwar Reddy D. NF-kappaB in acute pancreatitis: mechanisms and therapeutic potential. *Pancreatol* 2016;**16**:477–88.
 33. Watanabe T, Kudo M, Strober W. Immunopathogenesis of pancreatitis. *Mucosal Immunol* 2017;**10**:283–98.
 34. Jakkampudi A, Jangala R, Reddy R, Mitnala S, Rao GV, Pradeep R, et al. Acinar injury and early cytokine response in human acute biliary pancreatitis. *Sci Rep* 2017;**7**:15276.
 35. Sendler M, Weiss FU, Golchert J, Homuth G, Brandt C van den, Mahajan UM, et al. Cathepsin B-mediated activation of trypsinogen in endocytosing macrophages increases severity of pancreatitis in mice. *Gastroenterology* 2018;**154**:704–18.
 36. Gukovsky I, Gukovskaya A. Nuclear factor-kappaB in pancreatitis: Jack-of-all-trades, but which one is more important?. *Gastroenterology* 2013;**144**:26–9.
 37. Huang H, Liu Y, Daniluk J, Gaiser S, Chu J, Wang H, et al. Activation of nuclear factor-kappaB in acinar cells increases the severity of pancreatitis in mice. *Gastroenterology* 2013;**144**:202–10.
 38. Mederos MA, Reber HA, Girgis MD. Acute pancreatitis: a review. *JAMA* 2021;**325**:382–90.
 39. Lee PJ, Papachristou GI. New insights into acute pancreatitis. *Nat Rev Gastroenterol Hepatol* 2019;**16**:479–96.
 40. Hu Q, Yao J, Wu X, Li J, Li G, Tang W, et al. Emodin attenuates severe acute pancreatitis associated acute lung injury by suppressing pancreatic exosome mediated alveolar macrophage activation. *Acta Pharm Sin B* 2022;**12**:3986–4003.
 41. Wong DJ, Park DD, Park SS, Haller CA, Chen J, Dai E, et al. A PSGL-1 glycomimetic reduces thrombus burden without affecting hemostasis. *Blood* 2021;**138**:1182–93.
 42. André P, Spertini O, Guia S, Rihet P, Dignat-George F, Brailly H, et al. Modification of P-selectin glycoprotein ligand-1 with a natural killer cell-restricted sulfated lactosamine creates an alternate ligand for L-selectin. *Proc Natl Acad Sci U S A* 2000;**97**:3400–5.
 43. An G, Wang H, Tang R, Yago T, McDaniel JM, McGee S, et al. P-selectin glycoprotein ligand-1 is highly expressed on ly-6chi monocytes and a major determinant for ly-6chi monocyte recruitment to sites of atherosclerosis in mice. *Circulation* 2008;**117**:3227–37.
 44. Laszik Z, Jansen PJ, Cummings RD, Tedder TF, McEver RP, Moore KL. P-selectin glycoprotein ligand-1 is broadly expressed in cells of myeloid, lymphoid, and dendritic lineage and in some non-hematopoietic cells. *Blood* 1996;**88**:3010–21.
 45. Spertini O, Cordey AS, Monai N, Giuffrè L, Schapira M. P-selectin glycoprotein ligand 1 is a ligand for L-selectin on neutrophils, monocytes, and CD34⁺ hematopoietic progenitor cells. *J Cell Biol* 1996;**135**:523–31.
 46. Furie B, Furie BC. Role of platelet P-selectin and microparticle PSGL-1 in thrombus formation. *Trends Mol Med* 2004;**10**:171–8.
 47. Martinez M, Joffraud M, Giraud S, Baisse B, Bernimoulin MP, Schapira M, et al. Regulation of PSGL-1 interactions with L-selectin, P-selectin, and E-selectin: role of human fucosyltransferase-IV and -VII. *J Biol Chem* 2005;**280**:53.

48. Liu P, Gao C, Chen H, Vong CT, Wu X, Tang X, et al. Receptor-mediated targeted drug delivery systems for treatment of inflammatory bowel disease: opportunities and emerging strategies. *Acta Pharm Sin B* 2021;**11**:2798–818.
49. Phillips JW, Barringhaus KG, Sanders JM, Hesselbacher SE, Czarnik AC, Manka D, et al. Single injection of P-selectin or P-selectin glycoprotein ligand-1 monoclonal antibody blocks neointima formation after arterial injury in apolipoprotein e-deficient mice. *Circulation* 2003;**17**:2244–9.
50. Abdulla A, Awla D, Hartman H, Weiber H, Jeppsson B, Regner S, et al. Platelets regulate P-selectin expression and leukocyte rolling in inflamed venules of the pancreas. *Eur J Pharmacol* 2012;**682**:153–60.
51. Su Z, Xiao D, Xie F, Liu L, Wang Y, Fan S, et al. Antibody–drug conjugates: recent advances in linker chemistry. *Acta Pharm Sin B* 2021;**11**:3889–907.
52. Gibbs RA, Rogers J, Katze MG, Bumgarner R, Weinstock GM, Mardis ER, et al. Evolutionary and biomedical insights from the rhesus macaque genome. *Science* 2007;**316**:222–34.
53. Yoon SB, Hong H, Lim HJ, Choi JH, Choi YP, Seo SW, et al. A novel IRAK4/PIM1 inhibitor ameliorates rheumatoid arthritis and lymphoid malignancy by blocking the TLR/MYD88-mediated NF- κ B pathway. *Acta Pharm Sin B* 2023;**13**:1093–109.
54. Rakonczay Jr Z, Hegyi P, Takács T, McCarroll J, Saluja AK. The role of NF-kappaB activation in the pathogenesis of acute pancreatitis. *Gut* 2008;**2**:259–67.
55. Sundar V, Tamizhselvi R. Inhibition of Rb phosphorylation leads to H₂S-mediated inhibition of NF- κ B in acute pancreatitis and associated lung injury in mice. *Pancreatology* 2020;**4**:647–58.
56. Jaworek J, Szklarczyk J, Kot M, Górska M, Jaworek A, Bonior J, et al. Chemerin alleviates acute pancreatitis in the rat through modulation of NF- κ B signal. *Pancreatology* 2019;**19**:401–8.
57. Russo HM, Wickenheiser KJ, Luo W, Ohman MK, Franchi L, Wright AP, et al. P-selectin glycoprotein ligand-1 regulates adhesive properties of the endothelium and leukocyte trafficking into adipose tissue. *Circ Res* 2010;**107**:388–97.
58. Xiao Q, Li X, Li Y, Wu Z, Xu C, Chen Z, et al. Biological drug and drug delivery-mediated immunotherapy. *Acta Pharm Sin B* 2021;**11**:941–60.
59. Sultana DA, Zhang SL, Todd SP, Bhandoola A. Expression of functional P-selectin glycoprotein ligand 1 on hematopoietic progenitors is developmentally regulated. *J Immunol* 2012;**188**:4385–93.